RSC Advances

ROYAL SOCIETY OF CHEMISTRY

PAPER

View Article Online
View Journal | View Issue

Cite this: *RSC Adv.*, 2026, **16**, 14867

New sesquiterpenoids from *Bontia daphnoides*: antioxidant and antidiabetic evaluation

Amira Mohamed, †[a] Dalia El Amir, †[a] Maha M. Abdel-Fattah, [b] Mohamed A. Zaki, *[a] Rabab Mohammed *[a] and Marwa H. A. Hassan [a]

Bontia daphnoides, commonly known as "olive brush", is a medicinal plant traditionally used in the management of diabetes mellitus. The current study evaluated the phytochemical composition along with the antioxidant and antidiabetic activities of the hydroethanolic extract of *B. daphnoides* aerial parts. The plant extract was found to be rich in phenolics (85.67 ± 0.018 mg GAE per g) and flavonoids (13.109 ± 0.007 mg QE per g). Phytochemical investigation yielded several metabolites from the *n*-hexane fraction including dehydromyoporone (**1**), β-sitosterol (**2**), α-amyrin (**3**), and β-sitosterol glucoside (**4**). The dichloromethane fraction afforded two new γ-lactone-containing sesquiterpenes (**5**) and (**6**), while the *n*-butanol fraction provided 8-acetylharpagide (**7**), verbascoside (acteoside) (**8**), crenatoside (**9**), and apigenin-7-*O*-glucuronide (**10**). The hydroethanolic extract of the plant exhibited antioxidant capacity, with 2,2-diphenyl-1-picrylhydrazyl (DPPH) radical scavenging activity of 109.239 ± 0.429 mg AAE per g and phosphomolybdenum reducing power of 152.20 ± 0.053 mg AAE per g. Furthermore, it demonstrated potent inhibition of α-glucosidase (IC_{50} = 0.047 ± 0.001 mg mL^{-1}) and α-amylase (IC_{50} = 0.088 ± 0.003 mg mL^{-1}) enzymes, with activities comparable to or surpassing acarbose activities (IC_{50} = 0.072 ± 0.002 mg mL^{-1} and 0.092 ± 0.003 mg mL^{-1}, respectively). In alloxan-induced diabetic rats, oral administration of the plant extract (200 and 400 mg kg^{-1}, 21 days) reduced blood glucose levels and alleviated oxidative stress by increasing reduced glutathione (GSH) levels, decreasing malondialdehyde (MDA) levels, and improving liver histology. Collectively, these findings highlight *B. daphnoides* as a rich source of antioxidant and antidiabetic metabolites, supporting its traditional use and suggesting its potential for development of novel therapeutic agents against diabetes and its complications.

Received 2nd January 2026
Accepted 3rd March 2026

DOI: 10.1039/d6ra00038j

rsc.li/rsc-advances

1. Introduction

Diabetes mellitus (DM) is a prevalent chronic metabolic disorder characterized by persistent hyperglycemia and associated disturbances in carbohydrate, lipid, and protein metabolism. It is classified into four major types: type I (insulin-dependent DM), type II (non-insulin-dependent DM), gestational diabetes, and other specific forms, with type II being the most common. Hyperglycemia in type II DM results from multiple pathophysiological factors, including insulin resistance, impaired insulin secretion, increased hepatic glucose production, and altered incretin activity. Among these factors, the rapid enzymatic hydrolysis of complex carbohydrates by pancreatic α-amylase and intestinal α-glucosidases contributes to postprandial hyperglycemia by accelerating the breakdown and absorption of dietary carbohydrates, leading to sharp glucose spikes after meals.[1]

Inhibition of the digestive enzymes α-glucosidase and α-amylase slows carbohydrate digestion, thereby reducing the rate of glucose absorption into the bloodstream.[2] Although synthetic competitive inhibitors such as acarbose, voglibose, and miglitol are clinically effective,[3] ongoing pharmacological research seeks to identify novel inhibitors with improved efficacy and safety profiles. Several plant-derived compounds have shown significant α-glucosidase and α-amylase inhibitory activities, highlighting their potential as therapeutic agents for type II diabetes. Given the complex pathophysiology of DM and the limitations or adverse effects associated with current antidiabetic drugs,[4] there is an increased scientific interest for developing safer and more effective alternatives from natural sources.

In Trinidad and Tobago, modern traditional healers have been using a variety of medicinal plants for the management of diabetes, with significant therapeutic benefits that have been reported by users. The reported therapeutic benefits may even exceed the clinical benefits of those of conventional pharmaceuticals; for example, antidiabetic plants like *Morinda citrifolia*

[a]*Department of Pharmacognosy, Faculty of Pharmacy, Beni-Suef University, Beni-Suef 62514, Egypt. E-mail: mohamed.zaki@pharm.bsu.edu.eg; rababmohammed@pharm.bsu.edu.eg; rmwork06@yahoo.com; Tel: +20 1102424231; +20 1202442204*

[b]*Department of Pharmacology and Toxicology, Faculty of Pharmacy, Beni-Suef University, Beni-Suef 62514, Egypt*

† These authors contributed equally to this work.

are highlighted for their potential as effective and safe alternatives to conventional drugs, offering benefits such as minimal side effects and lower cost. Their mechanisms of action involve various bioactive compounds that can influence insulin secretion, glucose absorption, and utilization, potentially surpassing modern drug benefits in some cases.[5] One of these plants is *B. daphnoides* which has long been valued for its ability to lower blood sugar levels. Such ethnomedical claims need to be thoroughly verified by science in order to clarify the phytochemical profile of the plant, its bioactive mechanism, and its general effectiveness in managing diabetes.[5]

Bontia daphnoides L. (family Scrophulariaceae), is a shrub native to the West Indies and known locally as olive bush, zoliv, buttonwood, and kidney bush. Traditionally, various parts of this plant have been used to treat inflammation, insect bites, intestinal worms, ulcers, wounds, herpes, diabetes, hypertension, nephritis, jaundice, cough, colds, and fish poisoning.[6–8] Early phytochemical studies have identified epingaione as a major secondary metabolite with notable acaricidal and insecticidal activity, including toxicity against *Cylas formicarius* (LC_{50} = 20.8 μg per insect) and cytotoxicity against TE-671 sarcoma cells (50.8% inhibition) and SH-SY5Y neuroblastoma cells (79.2%).[9] The crude plant extracts have shown antiproliferative effects against MDA-MB-231 breast cancer and Hep-G2 liver cancer cell lines.[6] GC/MS analysis of the essential oils from leaves, flowers, fruits, and stems revealed variations in volatile constituents dominated by oxygenated sesquiterpenes. The sesquiterpenoid; dehydroepingaione, isolated from the lipophilic leaf fraction, along with oils from leaves and stems, exhibited strong antiviral activity against CoxB4 and HSV-1, whereas the flowers oil was less active.[10] The dichloromethane fraction showed moderate antiviral effects (EC_{50} = 332 and 290 μg mL^{-1} against HSV-1 and HAV-H10, respectively) while the total extract exhibited stronger antiviral activity (EC_{50} = 214 and 190 μg mL^{-1}, respectively).[11] Furthermore, endophytic *Nodulisporium* sp. isolated from Hawaiian *B. daphnoides* was reported to produce nodulisporic acid A and related derivatives which are potent systemic agents for tick and flea control in animals with *N-tert*-butyl nodulisporamide identified as an effective oral formulation.[12,13]

Despite these previous findings, comprehensive investigations into the chemical composition and pharmacological activities of *B. daphnoides*, particularly regarding its potential antidiabetic effects, remain limited. Given its traditional use in diabetes management and the growing demand for safe, plant-based therapeutic agents. This study aimed to characterize the phytochemical profile of *B. daphnoides* leaves through determination of total phenolic and total flavonoid contents, isolation and identification of secondary metabolites, and evaluation of antidiabetic, enzyme inhibitory, and antioxidant activities using both *in vitro* and *in vivo* models.

2. Material and methods

2.1. Plant material

Bontia daphnoides was collected from Giza Zoo, Giza, Egypt. The plant was taxonomically authorized by Prof. Dr Abdelhalim Mohamed (Plant Taxonomy Department, Agricultural Research Center, Giza, Egypt). A voucher specimen (BUPD-116-2021) was deposited at the Department of Pharmacognosy, Faculty of Pharmacy, Beni-Suef University. The aerial parts were separated from the freshly collected plant material, air-dried, powdered and stored in dry and tight containers till use.

2.2. General instruments and chemicals

For chromatographic separation, silica gel 60 (Sigma-Aldrich Chemicals, Darmstadt, Germany), and Sephadex LH-20 (0.25–0.1 mm, GE Healthcare Bio-Sciences AB SE 75184 Uppsala, Sweden) were used for column chromatography (CC). TLC plates (Fluka precoated silica gel F_{254}) were used for column monitoring. Solvents used for NMR analysis were MeOH-d_4 (CD_3OD), dimethyl sulphoxide-d_6 (DMSO-d_6), and chloroform-d ($CDCl_3$) were purchased from (Sigma-Aldrich, Germany). Bruker NMR spectrometer was used to acquire NMR data running at 400, and 100 MHz for ^1H and ^{13}C NMR and DEPTQ, respectively. Spectra were recorded relative to tetramethylsilane (Me_4Si) as the internal standard. Two-dimensional (2D) NMR experiments (HSQC and HMBC) were performed utilizing the pulse sequences from the Bruker user library. HR-ESI-MS data were obtained from a FTHRMS-Orbitrap (Thermo Finnigan) mass spectrometer. Multi-well spectrophotometer (fluorescence plate reader) was used for *in vitro* activities. Acarbose, alloxane, and glimepiride were purchased from Merck (Darmstadt, Germany) for *in vitro* and *in vivo* activities. Other solvents like ethanol, *n*-hexane, dichloromethane (DCM), ethyl acetate (EtOAc), methanol (MeOH), *n*-butanol were obtained from El-Nasr Company for Pharmaceuticals and Chemicals, Egypt. Other chemicals: aluminum chloride, ammonium molybdate, ascorbic acid (vitamin C), 2,2-diphenyl-1-picrylhydrazyl (DPPH), ferric chloride, Folin–Ciocalteu reagent, gallic acid, potassium acetate, quercetin, sodium carbonate, sodium phosphate, and sulfuric acid were purchased from Sigma-Aldrich Chemical Co.

2.3. Exploration of the hydroethanolic extract of *B. daphnoides* aerial parts

The dried powdered aerial parts of *B. daphnoides* (1.6 kg) were exhaustively extracted by cold maceration (6 × 8 L, each 48 h) with aqueous ethanol (80%), the collected hydroethanolic extract was dried under reduced pressure using rotary evaporator. The dry extract was suspended in water and successively partitioned with *n*-hexane, DCM, EtOAc and *n*-butanol. The *n*-hexane fraction (10 g) was subjected to silica gel column chromatography (CC) and *n*-hexane as a mobile phase with gradual increase in polarity using EtOAc 2.5% till 100%. Three main subfractions (**A–C**) were combined and evaporated separately under reduced pressure. Successive CCs were used for isolation of four metabolites: compound **1** (20 mg), compound **2** (48.9 mg), compound **3** (3.3 mg) and compound **4** (10 mg).

The DCM fraction (6 g) was treated in similar method using *n*-hexane and EtOAc with 10% gradual increase in polarity. Sub fraction **A** (0.6 g) was subjected to silica gel CC using and *n*-hexane as mobile phase with gradual increase in polarity using EtOAc 5% till 30% EtOAc. Subfraction **A1** was further purified

on Sephadex LH-20 CC and (80 : 20) MeOH : CH_2Cl_2 as mobile phase to afford compounds **5** and **6** as a mixture (5 mg). The *n*-butanol fraction (15 g) was subjected to polyamide CC and distilled H_2O as a mobile phase with 10% increments of MeOH up to 100%. Four main subfractions (**A–D**) were obtained. Successive CCs were used for isolation and purification of four metabolites: compound **7** (10.3 mg), compound **8** (37.7 mg), compound **9** (3 mg), and compound **10** (3 mg). The method of isolation in details is provided in the SI (page 4).

2.4. Spectroscopic data of compounds 5 and 6

The compounds were isolated as yellow oil isomeric mixture (3 : 1); with $R_f = 0.15$ in *n*-hexane : EtOAc (7 : 3). ^{1}H NMR (400 MHz, $CDCl_3$), DEPTQ NMR (100 MHz, $CDCl_3$) and 2D NMR spectroscopic data are displayed in (SI, Fig. S9–S12). ^{1}H NMR (400 MHz, $CDCl_3$) (δ ppm) of compound **5**: 7.04 (s, 1H, H-**4**″), 6.12 (s, 2H, H-3 & H-**5**″), 4.84 (br s, 1H, H-2′), 2.67 (s, 2H, H-1), 2.32 (m, 1H, H-**3**′a), 2.11 (s, 3H, H-**4**-methyl), 2.11 (m, 1H, H-4′), 2.00 (m, 1H, H-3′b), 1.90 (m, 1H, H-4′b), 1.88 (s, 3H, H-5), 1.34 (s, 3H, H-5′-methyl). ^{1}H NMR (400 MHz, $CDCl_3$) (δ ppm) of compound **6**: 6.12 (s, 2H, H-3* & H-5″*), 5.94 (s, 1H, H-**3**″), 4.72 (m, 1H, H-2′*), 2.70 (s, 2H, H-1*), 2.32 (m, 1H, H-3′a*), 2.11 (s, 3H, H-4-methyl*), 2.11 (m, 1H, H-4′a*), 2.00 (m, 1H, H-3′b*), 1.90 (m, 1H, H-4′b*), 1.88 (s, 3H, H-5*), 1.34 (s, 3H, H-5′-methyl*).

DEPTQ NMR of compound **5** (100 MHz, $CDCl_3$) (δ ppm): δ_C 199.3 (C-2), 170.9 (C-2″), 156.3 (C-4), 144.1 (C-4″), 139.4 (C-**3**″), 125.2 (C-3), 98.2 (C-**5**″), 83.5 (C-**5**′), 74.3 (C-**2**′), 54.5 (C-1), 37.2 (C-**4**′), 31.3 (C-**3**′), 28 (C-5), 26.8 (C-5′-methyl), 21.1 (C-4-methyl). DEPTQ NMR of compound **6** (100 MHz, $CDCl_3$) (δ ppm): δ_C 199.2 (C-2*), 169.19 (C-2″*), 156.37 (C-4*), 125.3 (C-3*), 117.1 (C-3″*), 97.6 (C-5″*), 83.4 (C-5′*), 73.0 (C-2′*), 54.8 (C-1*), 36.7 (C-4′*), 31.3 (C-3′*), 27.9 (C-5*), 26.6 (C-5′-methyl*), 21.0 (C-4-methyl*). They exhibited a molecular ion peak at *m*/*z* 281.13849 $[M + H]^+$ in HR-ESI-MS positive ion mode corresponding to the molecular formula $C_{15}H_{20}O_5$ and *m*/*z* 303.12033 $[M + Na]^+$, corresponding to the molecular formula $C_{15}H_{19}O_5Na$.

2.5. Total flavonoid content (TFC)

Total flavonoid content (TFC) in the hydroethanolic extract was determined using the aluminum chloride colorimetric method, according to the procedure by ref. 14. A 0.5 mL aliquot of the extract (1 mg mL^{-1}) was mixed with 1.5 mL of methanol. Subsequently, 0.1 mL of 10% aluminum chloride and 0.1 mL of 1 M potassium acetate were added, followed by 2.8 mL of distilled water. The reaction mixture was incubated for 30 minutes at room temperature before measuring the absorbance at 415 nm. A calibration curve was constructed using quercetin as a standard, with concentrations ranging from 4–12 μg mL^{-1}. The TFC was then calculated and expressed as milligrams of quercetin equivalent (mg QE) per gram of dry extract.

2.6. Total phenolic content (TPC)

Total phenolic content (TPC) was quantified using the Folin–Ciocalteu method, as described by ref. 15. A 0.1 mL aliquot of the hydroethanolic extract (1 mg mL^{-1}) was mixed with 0.75 mL of Folin–Ciocalteu reagent, which had been diluted 10-folds with distilled water. The mixture was allowed to react for 5 minutes at room temperature, after which 0.75 mL of a 6% sodium carbonate solution was added. The absorbance of the final reaction mixture was measured at 725 nm after a 90 minutes of incubation. A standard calibration curve was constructed using gallic acid, with concentrations ranging from 20 to 120 μg mL^{-1}. TPC was calculated from this curve and expressed as milligrams of gallic acid equivalent (mg GAE) per gram of dry extract weight.

2.7. Biological activities

2.7.1. *In vitro* antioxidant activities of *B. daphnoides* hydroethanolic extract

2.7.1.1. DPPH (2,2-diphenyl-1-picrylhydrazyl) free radical scavenging assay. The free radical scavenging potential of *B. daphnoides* hydroethanolic extract (1 mg mL^{-1}) was determined using the 2,2-dipheny-1-picrylhydrazyl (DPPH) assay according to ref. 16. Briefly, 50 μL of the sample solution was mixed with 950 μL of methanolic DPPH solution (3.4 mg per 100 mL). The reaction mixture was incubated in the dark for 1 h at 37 °C. The free radical scavenging potential of the extract was determined by the decrease in absorbance of the DPPH radical, that was measured at 517 nm using UV-visible spectrophotometer (Agilent 8453, Germany). The reduction in absorbance corresponds to the disappearance of the initial purple color of the DPPH radical. Ascorbic acid was used as a positive control. The DPPH radical scavenging activity was calculated using the following formula: Scavenging activity (%) = $(A_{control} - A_{sample})/(A_{control}) \times 100$; where $A_{control}$ is the absorbance of the control reaction (containing all reagents except the extract), and A_{sample} is the absorbance of the extract.

2.7.1.2. Phosphomolybdenum assay. Total antioxidant capacity was determined using phosphomolybdenum assay as described by ref. 17. An aliquot of 0.1 mL of the sample solution was added to 1 mL of reagent solution, which consisted of 28 mM sodium phosphate, 0.6 M sulfuric acid and 4 mM ammonium molybdate. The mixture was then incubated in a water bath (95 °C) for 90 min. After incubation, the sample was cooled to room temperature, and the absorbance was recorded at 765 nm.

2.7.2. *In vitro* antidiabetic activity of *B. daphnoides* hydroethanolic extract. The *in vitro* antidiabetic activity of the *B. daphnoides* hydroethanolic extract was evaluated by assessing its inhibitory effects on carbohydrate-metabolizing key enzymes, specifically α-glucosidase and α-amylase. Both α-glucosidase and α-amylase are crucial digestive enzymes, where α-amylase breaks down complex starch molecules into smaller sugars by hydrolyzing the α-1,4-glycosidic linkages[18] and α-glucosidase, located in the small intestine, further breaks down these smaller carbohydrates into absorbable glucose.[19] Inhibiting these enzymes makes the digestion and absorption of carbohydrates slower, which helps to control the postprandial increase in blood glucose levels. This makes their inhibition a validated and effective strategy for managing metabolic disorders like diabetes and obesity.

2.7.2.1. α-Glucosidase inhibitory assay. The α-glucosidase inhibitory assay was performed in accordance with the protocol provided by the Bio-vision assay kit (catalog #K938). In a clear 96-well plate, the plant extract and the reference drug (acarbose), were prepared. For each well, 10 μL of the sample (extract or acarbose) was combined with 10 μL of the assay buffer and 10 μL of the enzyme solution (prepared by diluting 2 μL of α-glucosidase with 38 μL of α-glucosidase assay buffer). The total volume was adjusted to 80 μL with the buffer, and the mixture was incubated at room temperature for 15–20 minutes. After the incubation period, 20 μL of the enzyme substrate, *p*-nitrophenyl-α-D-glucopyranoside (PNPG), was added to each well. The absorbance was then recorded at 410 nm to quantify the enzymatic activity. The IC_{50} values for both the extracts and acarbose were subsequently calculated from the data.[20,21]

2.7.2.2. α-Amylase inhibitory assay. The inhibitory potential of the extract and the reference drug (acarbose), was assessed using an *in vitro* α-amylase inhibition assay, following the protocol of Bio-vision assay kit (catalog #K482). In a 96-well microplate, 50 μL of the sample (extract or standard) was combined with 50 μL of the enzyme solution. The mixture was incubated at room temperature for 10 minutes to allow for binding. Subsequently, 50 μL of a starch solution was added, and the reaction was allowed to proceed for 3 minutes. To stop the enzymatic reaction, 50 μL of 3,5-dinitrosalicylic acid (DNS) reagent was added, and the plate was then boiled in a water bath at 85–90 °C for 10 minutes. The mixture was cooled to room temperature, and the absorbance was measured at 405 nm to quantify the remaining substrate.[18,22]

2.7.3. Acute toxicity study of *B. daphnoides* hydroethanolic extract. This study was conducted according to the Organization for Economic Co-operation and Development (OECD) no. 420.[23]

Thirty male Swiss albino mice (20–25 g) were used. The animals were acclimatized for seven days before the experiment and fasted overnight prior to dosing. They were randomly divided into five groups ($n = 6$). The control group received the vehicle only (0.3% carboxymethyl cellulose, CMC), while the other four groups each received a single oral dose of the extract (0.001–1 g kg^{-1}) suspended in 0.3% CMC. The animals were observed for 48 h to monitor mortality and possible signs of toxicity. Parameters assessed included changes in ear and skin appearance, eyes, circulatory and respiratory function, autonomic responses, and motor activity. Signs of toxicity such as convulsions, tremors, diarrhea, salivation, lethargy, sleep, coma, and behavioral changes were also recorded.

2.7.4. *In vivo* assessment of the antidiabetic activity of *B. daphnoides* hydroethanolic extract

2.7.4.1. Animals. Healthy adult male albino Wistar rats (150–170 g weight) were housed in the animal house of Faculty of Pharmacy, Beni-Suef University. The central animal house conditions were well ventilated, the temperature kept at 25 ± 2 °C, with relative humidity of 50–60%, 12 h dark/light cycle and were provided with water and regular laboratory food. Rats were kept in plastic hygienic cages during the experimental period. The study was carried out in compliance with the approved Ethical Guidelines for the Care and Use of Experimental Animals by Beni-Suef University Ethical Committee (approval no.: FPHBSU IACUC-025-006).

2.7.4.2. Experimental design. The animals were divided into two groups after accommodation. The first group ($n = 5$) used as a normal control and administered 0.3% CMC as a vehicle. The second group of 35 rats that had been intraperitoneal administered a single dose of alloxan at a dosage of 150 mg kg^{-1} body weight after overnight fasting.[24] The blood glucose levels of the rats were checked after seven days, and those with blood glucose levels above 200 mg dL^{-1} were considered diabetic.

After induction of diabetes with alloxan, the animals were left for a stabilization period of 7 days to allow the development of a stable hyperglycemic state. During this period, blood glucose levels were monitored, and only rats that consistently exhibited fasting blood glucose levels ≥200 mg dL^{-1} were considered to have established (stabilized) diabetes and were included in the study. Diabetic stabilization "refers to the period following alloxan administration during which hyperglycemia becomes persistent and stable, indicating successful destruction of pancreatic β-cells and establishment of the diabetic state". After diabetic stabilization, twenty-eight male rats were divided into four subgroups consisting of seven rats each; subgroup I: diabetic rates were kept as positive control group received 0.3% CMC as a vehicle. Subgroup II: is a standard group received glimepiride (5 mg kg^{-1}, body weight) for 3 weeks. Subgroup III: diabetic rates administrated plant extract 200 mg per kg body weight per day. Subgroup IV: diabetic rates administrated plant extract 400 mg per kg body weight per day for three weeks.

After the experiment period, rats were given anesthesia 24 hours following the final treatment in order to obtain a blood sample from the retro-orbital plexus, left to clot, then centrifuged to separate serum samples, kept at −20 °C for assessment of blood glucose, insulin, and oxidative stress markers as reduced glutathione (GSH) and malondialdehyde (MDA) levels. Rats then euthanized with rapid cervical dislocation, and livers were dissected and fixed in 10% formal saline for histopathological study.

2.7.4.3. Assessment of biochemical markers

2.7.4.3.1. Determination of blood glucose and insulin levels. Blood glucose level was assessed using Glucometer (GlucoDr, Korea)[25,26] and serum insulin level was assessed using a specific ELISA kit (cat. no.: ARG80655) following the manufacturer's instructions.

2.7.4.3.2. Determination of serum oxidative stress markers (GSH and MDA). Malondialdehyde (MDA) was typically employed as a measure of oxidative stress while, reduced glutathione level (GSH) was employed as an example for non-enzymatic antioxidants. The serum levels of GSH and MDA were assessed using a specific ELISA kit (Bio-Diagnostic Co. – Cairo, Egypt), following the manufacturer's instructions.

2.7.4.3.3. Histopathological analysis of liver tissue. Liver tissue samples were fixed in 10% formal saline, dehydrated through a graded ethanol series (70%, 80%, 90%, 95%, and 100%), cleared in xylene, and embedded in Paraplast tissue embedding medium. A microtome was used to cut liver slices

(3–5 μm), which were then stained with hematoxylin and eosin (H&E) and examined under a microscope.[27]

2.8. Statistical analysis

All the data were expressed as mean ± standard deviation (SD) from three experiments, the data of TPC, TFC, and antioxidant activity calculated from linear calibration curve plotted by excel software using different concentrations of the standards. All results of the *in vivo* antidiabetic study are presented as mean ± standard error of the mean (SEM). Statistical analyses were conducted using GraphPad Prism software, version 8.4.3 (published by GraphPad Software, Inc. (now part of Dotmatics); release date June 16, 2020). Differences among groups were assessed by one-way analysis of variance (ANOVA), followed by Tukey's *post hoc* test. A *P*-value of less than 0.05 was considered statistically significant.

3. Results and discussion

3.1. TPC and TFC

The total phenolic content (TPC) of *B. daphnoides* aerial parts hydroethanolic extract was determined using the Folin–Ciocalteu assay. As shown in Table 1, the TPC of the extract was 85.67 ± 0.018 mg GAE per g of dry extract, with the results expressed as milligrams of gallic acid equivalent per gram of dry extract.

While the total flavonoid content (TFC) of the plant extract was determined using the aluminum chloride colorimetric method, with the results expressed as milligrams of quercetin equivalent (mg QE) per gram of dry extract. As shown in Table 1, the TFC of the plant was found to be 13.109 ± 0.007 mg QE per g.

3.2. Identification and structure elucidation of the isolated compounds from *B. daphnoides* hydroethanolic extract

The biological activities observed for the hydroethanolic extract encourage further investigation of their active constituents; consequently, a phytochemical study was conducted on the *n*-hexane, dichloromethane and *n*-butanol fractions of *B. daphnoides*. A total of ten metabolites (**1–10**) were isolated and identified through spectral data analysis and comparison with previously reported literature. The chemical structures are presented in Fig. 1. From the *n*-hexane fraction, one oxygenated sesquiterpene, two sterols, and one triterpene were obtained, namely dehydromyoporone (**1**), previously reported from *B. daphnoides*[11] (Thabet, Ayoub *et al.*[11] 2025), β-sitosterol (**2**)[28,29] (Li, Huang *et al.* 2009, Elhawary, Hassan *et al.* 2023), β-sitosterol glucoside (**4**)[30,31] (Peshin and Kar 2017, Renda, Kadıoğlu *et al.* 2021), α-amyrin (**3**)[32,33] (Miranda, Silva *et al.* 2006, Naidu, Kumar *et al.* 2012), respectively. The dichloromethane fraction afforded mixture of two new γ-lactone-containing sesquiterpenes (**5**) and (**6**). In addition, the *n*-butanol fraction yielded one iridoid glucoside, two phenylethanoid glycosides, and one flavonoid glycoside, isolated for the first time from *B. daphnoides*: 8-acetylharpagide (**7**)[34,35] (Shin, Lee *et al.* 2020, Gao, Le Ba *et al.* 2021), verbascoside (acteoside) (**8**)[36] (Delazar, Asnaashari *et al.* 2019), crenatoside (**9**)[37,38] (da Silva, Rodrigues *et al.* 2014, Shen, Li *et al.* 2015), and apigenin-7-*O*-glucuronide (**10**)[39,40] (Luca, Czerwińska *et al.* 2019, Du, Xiong *et al.* 2024), respectively. The corresponding spectral data for all the identified compounds are provided in the SI section (Fig. S1–S22).

Compounds (**5** and **6**) were obtained as yellowish oily mixture of two compounds in 3 : 1 ratio. Both compounds exhibited similar mass spectra with the same molecular formula of $C_{15}H_{20}O_5$ as determined by HR-ESI-MS data (SI: Fig. S13), *m*/*z* 281.13849 $[M+H]^+$ (calculated for $C_{15}H_{21}O_5$) and *m*/*z* 303.12033 $[M + Na]^+$, corresponding to the molecular formula $C_{15}H_{19}O_5Na$, indicating the presence of six double bond equivalents (DBE).

Analysis of the ^{1}H NMR and DEPTQ NMR spectra, in combination with 2D-NMR experiments (HSQC, HMBC) (Table 2) (SI: Fig. S9–S12) indicated the presence of a hydroxy-α,β-unsaturated-γ-lactone ring with overlapping signals. Their NMR data closely resembled those of previously reported compounds[41,42] except for the presence of an olefinic proton signal at δ_H 6.12 (s, 2H, H-3 and H-3*) and two allylic methyl carbons at δ_C 28.0, 27.9 (C-5 and C-5*) and 21.1, 21.0 (C-4-methyl and C-4-methyl*) indicating the presence of an enone system. The ^{1}H NMR data of both compounds showed minimal variation, displaying characteristic resonances of two olefinic methine protons at δ_H 7.04 (s, 1H, H-**4**″), 6.12 (s, 4H, H-3, H-**5**″, H-**5**″*, and H-3*), 5.94 (s, 1H, H-**3**″*), three methyl protons at δ_H 2.11 (s, 6H, H-4-methyl and H-4-methyl*), 1.88 (s, 6H, H-5 and H-5*), 1.34 (s, 6H, H-5′-methyl and H-5′-methyl*), four methine protons at δ_H 6.12 (s, 2H, H-**5**″, H-**5**″*), 4.84 (br s, 1H, H-**2**′) and 4.72 (m, 1H, H-**2**′*), and six methylene's protons at δ_H 2.00–2.32 (m, 4H, H-**3**′ and H-**3**′*), δ_H 1.90–2.11 (m, 4H, H-**4**′ and H-**4**′*), δ_H 2.67 (s, 2H, H-1) and δ_H 2.70 (s, 2H, H-1*). The DEPTQ NMR spectrum revealed 28 signals. Of these, 13 signals were assigned to one compound, the other 13 signals belong to the second compound, and 2 signals were common to both compounds. The carbon resonances included nine quaternary carbons at δ_C 199.3, 199.2 (C-2 and C-2*), 170.9, 169.1 (C-**2**″ and C-**2**″*), 156.39, 156.37 (C-4 and C-4*), 139.4 (C-**3**″ and C-**4**″*), 83.5, 83.4 (C-**5**′ and C-**5**′*), eight methines at δ_C 117.1 (C-**3**″), 144.1 (C**4**″*), 125.3, 125.2 (C-3 and C-3*), 98.2, 97.6 (C-**5**″ and C-**5**″*), 74.3, 73.0 (C-**2**′ and C-**2**′*), five methylene's at δ_C 54.8, 54.5 (C-1 and C-1*), 37.2, 36.7 (C-**4**′ and C-**4**′*), 31.1 (C-**3**′), and six methyl's at δ_C 28.0, 27.9 (C-5 and C-5*), 26.8, 26.6 (C-5′-methyl and 5′-methyl*), 21.1, 21.0 (C-4-methyl and C-4-methyl*).

HMBC revealed key correlations (SI Fig. S12) supporting the structural features of the two compounds. Protons H-**4**″ and H-**3**″ exhibited correlations with C-2″, confirming their

Table 1 Total phenolic and flavonoid contents of *B. daphnoides* aerial parts hydroethanolic extract

	TPC[a] (mg GAE per g)	TFC[b] (mg QE per g)
B. daphnoides	85.67 ± 0.018	13.109 ± 0.007

[a] TPC: total phenolic content, mg gallic acid equivalent in 1 g of dry extract. [b] TFC: total flavonoid content, mg quercetin equivalent in 1 g of dry extract.

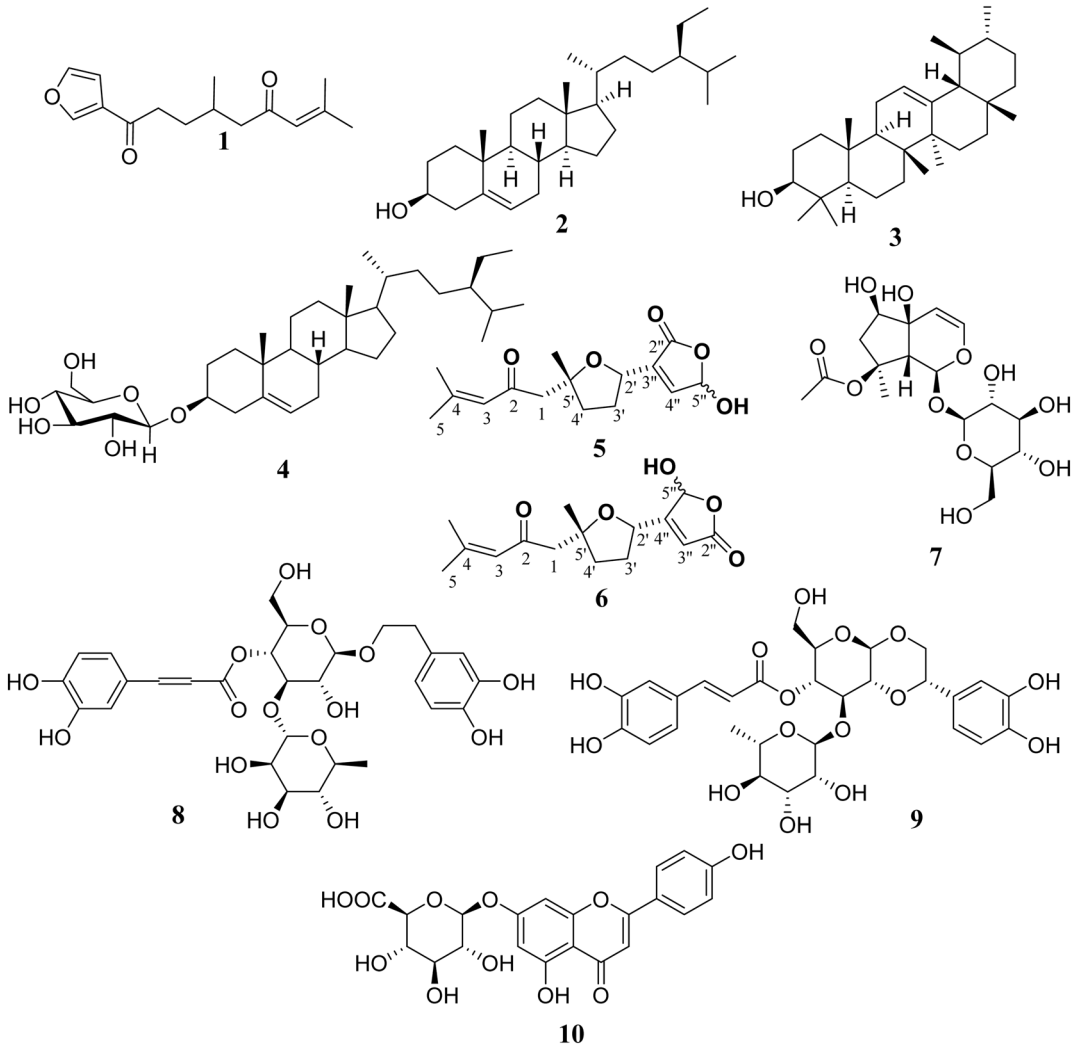

Fig. 1 Structures of the isolated metabolites (**1–10**) from the hydroethanolic extract of *B. daphnoides* aerial parts.

Table 2 ^{1}H NMR (400 MHz) and DEPT-Q (100 MHz) spectroscopic data for compounds **5** and **6** in $CDCl_3$

	Compound **5**			Compound **6**		
Position	δ_H, mult., J	δ_C, type	HMBC	δ_H, mult., J	δ_C, type	HMBC
2″	—	170.9, C		—	169.19*, C	
3″	—	139.4, C		5.94 (s)	117.1, CH	C-2″
4″	7.04 (s)	144.1, CH	C-2″	—	139.4, C	
5″	6.12 (s)	98.2, CH	C-2″	6.12 (s)	97.6, CH*	C-2″
2′	4.84 (br s)	74.3, CH		4.72 (m)	73.0, CH	
3′	2.00–2.32 (m)	31.3, CH_2	C-2′, C-4′, C-5′, C-1, C-5′-methyl	2.00–2.32 (m)	31.3, CH_2	C-2′, C-4′, C-5′, C-1, C-5′-methyl
4′	1.90–2.11 (m)	37.2, CH_2	C-2′, C-4′, C-5′, C-1, C-5′-methyl	1.90–2.11 (m)	36.7, CH_2	C-2′, C-3′, C-5′, C-1, C-5′-methyl
5′	—	83.5, C		—	83.4, C	
1	2.67 (s)	54.5, CH_2	C-4′, C-5′, C-2, C-3, C-5′-methyl	2.70 (s)	54.8, CH_2	C-4′, C-5′, C-2, C-3, C-5′-methyl
2	—	199.3, C		—	199.2, C	
3	6.12 (s)	125.2, CH	C-2, C-5, C-4-methyl	6.12 (s)	125.3, CH	C-2, C-5, C-4-methyl
4	—	156.3, C		—	156.3, C	
5	1.88 (s)	28.0, CH_3	C-3, C-4, C-4-methyl	1.88 (s)	27.9, CH_3	C-3, C-4, C-4-methyl
4-Methyl	2.11 (s)	21.1, CH_3	C-2, C-3, C-4, C-5	2.11 (s)	21.0, CH_3	C-2, C-3, C-4, C-5
5′-Methyl	1.34 (s)	26.8, CH_3	C-2″, C-4′, C-5′, C-1	1.34 (s)	26.6, CH_3	C-2″, C-4′, C-5′, C-1

positioning within the same ring system. The presence of a second ring was established by the correlations of H-3′ with C-4′ and C-5′. Additionally, correlations between H-5′-methyl and C-4′/C-5′ verified the attachment of a methyl group to the tetrahydrofuran moiety. Further correlations of H-1 with C-4′, C-5′, C-2, C-3, and C-5′-methyl substantiated the presence of a penten-3-one side chain. Moreover, correlations between H-4-methyl and C-2, C-3, C-4, and C-5, together with correlations between H-5 and C-3, C-4, and C-4-methyl, further supported the structural assignment. In summary, structures of compounds (**5**) and (**6**) were elucidated as a pair of new regio isomeric γ-lactone sesquiterpenes as shown in Fig. 1 and named as [(2′*S*,5′*R*)-4-methyl-1-(5′-methyl-2′,3′,4′,5′-tetrahydro [2′,3″-bifuran-(5″-hydroxyfuran-2″-one)]-5′yl)-2-oxopent-3-en-1yl] (**5**) and [(2′*S*,5′*R*)-4-methyl-1-(5′-methyl-2′,3′,4′,5′-tetrahydro [2′,4″-bifuran-(2″-hydroxyfuran-5″-one)]-5′yl)-2-oxopent-3-en-1yl] (**6**).

3.3. Biological activities

3.3.1. *In vitro* antioxidant activity. The antioxidant potential of the hydroethanolic extract was assessed using two distinct assays: the DPPH free radical scavenging assay and the total antioxidant capacity (TAC) phosphomolybdate assay. The results for both were expressed as milligrams of ascorbic acid equivalent per gram of dry extract (mg AAE per g dry extract), as shown in Table 3.

The results of the DPPH assay were calculated as 109.239 ± 0.429 mg AAE per g of dry extract. While the results of phosphomolybdate assay showed that each gram of the extract had a total antioxidant capacity of 152.20 ± 0.053 mg of ascorbic acid. Early studies demonstrated that verbascoside-enriched ethanol extracts of *Clerodendrum glandulosum* leaves exhibited potent DPPH radical scavenging activity, with an IC_{50} value of 39.51 ± 0.51 μg mL^{-1}, verbascoside has been consistently reported as an effective free radical scavenger, primarily due to its ability to participate in proton and/or electron transfer reactions with free radicals.[43] Another report revealed that verbascoside isolated from *Plantago major* significantly scavenge both DPPH and superoxide radicals with (IC_{50}, 11.27 μM and 1.51 μM, respectively).[44] As well the structurally related phenylethanoid glycosides such as crenatoside showed remarkable antioxidant potential, achieving 99.9% radical scavenging activity at 1.0 mg mL^{-1} and 93.7% activity even at 0.005 mg mL^{-1}, surpassing the standard antioxidants Trolox and vitamin C.[37] Moreover apigenin-7-*O*-β-D-glucuronide methyl ester previously isolated from the ethyl acetate extract of *Manilkara zapota* leaves exhibited significant DPPH and NO free radical inhibiting activity with IC_{50} values of 36.38 μg mL^{-1} and 29.74 μg mL^{-1} at 100 μg mL^{-1}, whereas the standards, ascorbic acid, and 3,5-di-*tert*-butyl-4-hydroxytoluene exhibited IC_{50} values of 4.49 μg mL^{-1} and 3.93 μg mL^{-1}, respectively at 10 μg mL^{-1}.[45] Therefore, it can be concluded that the antioxidant activity of the extract of *B. daphnoides* could be primarily attributable to the presence of verbascoside, crenatoside and apigenin-7-*O*-β-D-glucuronide, which were isolated in the present study.

3.3.2. *In vitro* antidiabetic activity. The results of α-glucosidase assay in Table 4, demonstrated potent α-glucosidase inhibitory activity with an IC_{50} of 0.047 ± 0.001 mg mL^{-1}. This activity was comparable to that of the reference standard, acarbose, which exhibited an IC_{50} of 0.072 ± 0.002 mg mL^{-1}. As well the results of α-amylase assay in Table 4, revealed a notable inhibitory effect on α-amylase with an IC_{50} of 0.088 ± 0.003 mg mL^{-1}. This activity was comparable to the standard drug, acarbose, which had an IC_{50} of 0.092 ± 0.003 mg mL^{-1}. Previous investigations have emphasized the inhibitory potential of verbascoside against carbohydrate-hydrolyzing enzymes, particularly α-glucosidase and α-amylase. Notably, verbascoside has been reported to exhibit stronger α-glucosidase inhibition than the reference drug acarbose.[46] For instance, verbascoside isolated from *Clerodendrum bungei* roots showed an IC_{50} of 0.5 ± 0.03 nM, compared with acarbose (IC_{50} = 14.4 ± 0.3 mM).[47] Similarly, verbascoside isolated from *Ruellia tuberosa* leaves inhibited α-glucosidase with an IC_{50} of 69.3 ± 0.2 μg mL^{-1},[48] while that obtained from *Monochasma savatieri* exhibited significant activity (IC_{50} = 0.5 ± 0.03 mM *vs.* acarbose IC_{50} = 14.4 ± 0.3 mM).[49] Moreover, a verbascoside-enriched ethanol extract of *Clerodendrum glandulosum* displayed potent inhibition of α-glucosidase and α-amylase, with IC_{50} values of 195.13 ± 3.26 μg mL^{-1} and 346.39 ± 5.04 μg mL^{-1}, respectively.[43] In addition, 8-acetylharpagide from *Caryopteris incana* showed notable α-glucosidase inhibition (IC_{50} = 1.89 ± 0.7 mM) compared to acarbose (IC_{50} = 3.49 ± 0.15 mM).[50] These results suggested that the *B. daphnoides* hydroethanolic extract demonstrated comparable or slightly superior inhibitory efficacy against α-amylase and α-glucosidase compared to the standard drug, acarbose. These results highlight its potential as a natural α-amylase and α-glucosidase inhibitor for managing postprandial hyperglycemia.

3.3.3. Acute toxicity. Oral administration of a single dose of different concentrations of *B. daphnoides* hydroethanolic extract

Table 3 Antioxidant activity of the hydroethanolic extract of *B. daphnoides* aerial parts using DPPH and phosphomolybdenum assay[a]

	mg AAE per g	
	DPPH	TAC
B. daphnoides	109.239 ± 0.429	152.20 ± 0.053

[a] DPPH: 2,2-diphenyl-1-picrylhydrazyl, TAC: total antioxidant capacity, AAE: ascorbic acid equivalent.

Table 4 Results of *in vitro* α-glucosidase, and α-amylase inhibitory activities of *B. daphnoides* aerial parts hydroethanolic extract[a]

	IC_{50} (mg mL^{-1})	
Extract	α-Glucosidase	α-Amylase
B. daphnoides	0.047 ± 0.001	0.088 ± 0.003
Acarbose®	0.072 ± 0.002	0.092 ± 0.003

[a] Each value is presented as means ± SEM, n = 3. IC_{50}, half-maximal inhibitory concentration; SEM, standard error of mean.

(0.001, 0.01, and 1 g per kg body weight) to albino mice groups did not induce any mortality during the first 48 h, compared to the negative control. No deaths or signs of toxicity were observed at doses up to 1 g kg^{-1}, indicating that the extract is non-toxic and safe at this concentration.

3.3.4. *In vivo* antidiabetic activity

3.3.4.1. Effect on blood glucose and serum insulin levels. The administration of alloxan in a dose of 150 mg kg^{-1}, i.p. significantly increased blood glucose level and decreased insulin level as compared to normal rats, that came in comply with previous studies as alloxan induced diabetes by selectively destroying pancreatic beta cells, leading to insulin deficiency and hyperglycemia.[51,52] While the administration of glimepiride, used as the standard drug, produced a significant hypoglycemic effect compared with the diabetic control group, consistent with its mechanism as a sulfonylurea insulin secretagogue. It works by stimulating the pancreas to release more insulin, helping the body utilize glucose more effectively.[53] Data presented in Fig. 2 reveals that the hydroethanolic extract *B. daphnoides* interestingly, in the two dose levels, 200 and 400 mg kg^{-1}, showed a significant attenuation in blood glucose level, although, for insulin measurement, *B. daphnoides* extract didn't show improvement in insulin secretion. Early data revealed that the verbascoside-enriched ethanol extract of *Marrubium vulgare* demonstrated significant antidiabetic activity, producing approximately a 50% reduction in blood glucose levels at a dose of 100 mg kg^{-1}.[54] Similarly, echinacoside and verbascoside (acteoside), the major constituents of *Cistanche tubulosa* stem extract (Orobanchaceae), were reported to enhance glucose tolerance and lower blood glucose levels in mice at doses of 250–500 mg kg^{-1}.[55] Furthermore, 8-*O*-acetylharpagide, previously isolated from *Scrophularia deserti*, was shown to reduce blood glucose levels by 17.0% after 1 h and 29.0% after 2 h in alloxan-induced diabetic mice.[56] Based on these earlier studies, it can be concluded that the effect of *B. daphnoides* extract is primarily attributable to the presence of verbascoside and 8-*O*-acetylharpagide where both were isolated in the present study.

3.3.4.2. Effect on serum antioxidants and oxidative stress biomarkers. Oxidative stress, which is caused by an imbalance between the production of reactive oxygen species (ROS) and antioxidant defense mechanisms, plays a critical role in the development and progression of DM and its complications. Elevated blood glucose levels in diabetic individuals enhance ROS generation, which can impair insulin secretion from pancreatic β-cells and induce insulin resistance in peripheral tissues.[57] Antioxidants protect β-cell function, enhance insulin sensitivity, and improve glucose uptake and utilization.[58,59] Furthermore, such compounds can modulate key signaling pathways involved in glucose metabolism, thereby contributing to glycemic control.[59] In the current study, the *B. daphnoides* extract treatment exhibited a significant antioxidant effect compared to the untreated diabetic group represented by a significant decrease in GSH levels and a concurrent increase in MDA levels compared to healthy controls. The low-dose group B3 (200 mg kg^{-1}) demonstrated a significant increase in GSH and a decrease in MDA levels, which aligns with its previously discussed hypoglycemic effects (Fig. 3). However, the higher dose of *Bontia daphnoides* (B4) (400 mg kg^{-1}) failed to produce a significant improvement in GSH levels compared to the diabetic group. This finding may be attributed to a dose-dependent biphasic (hormetic) response, a well-recognized phenomenon in phytotherapy, where moderate doses enhance antioxidant defenses, whereas higher doses may exert diminished or pro-oxidant effects. Excessive phytochemical concentrations can increase reactive oxygen species generation, interfere with glutathione synthesis, or inhibit glutathione-related enzymes, ultimately blunting antioxidant efficacy. Similar observations have been reported with several plant-derived antioxidants in experimental diabetes, where higher doses failed to improve or even worsened oxidative stress markers. Thus, the absence of a significant increase in GSH levels in the B4 group suggests that the antioxidant effect of

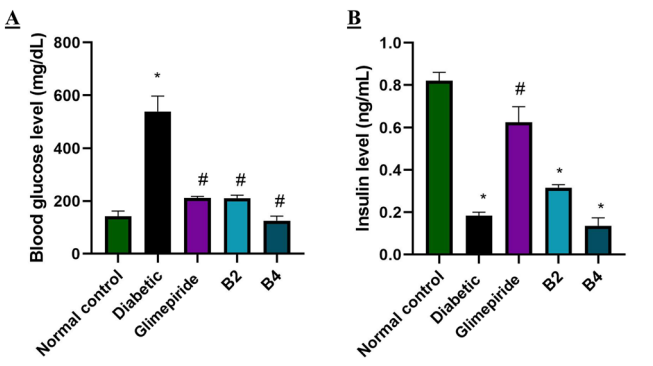

Fig. 2 Effect of the hydroethanolic extract of *B. daphnoides* aerial parts on blood glucose and serum insulin levels. (A) Blood glucose level (mg dL^{-1}), (B) insulin level (ng mL^{-1}). B2: *B. daphnoides* at dose 200 mg kg^{-1}, B4: *B. daphnoides* at dose 400 mg kg^{-1}. Each bar represents mean ± S.E.M. ($n = 5$). One-way ANOVA statistical test was conducted to analyze significant difference among tested groups followed by Tukey–Kramer multiple comparisons test. *$P < 0.05$ *versus* normal control group. #$P < 0.05$ *versus* diabetic control group.

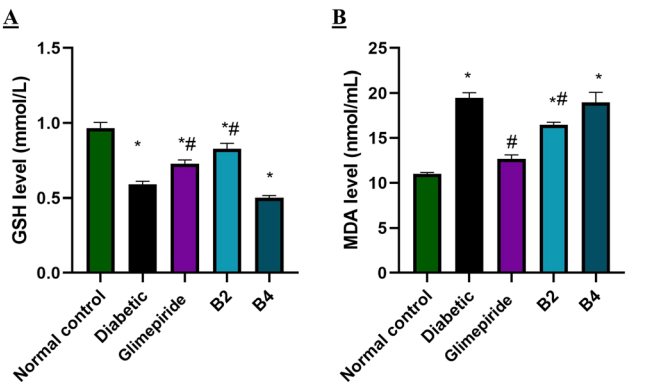

Fig. 3 Hydroethanolic extract of *B. daphnoides* aerial parts on serum antioxidants and oxidative stress biomarkers. (A) Serum reduced glutathione (GSH) level (mmol L^{-1}), (B) serum malondialdehyde (MDA) level (nmol mL^{-1}). B2: *B. daphnoides* at dose 200 mg kg^{-1}, B4: *B. daphnoides* at dose 400 mg kg^{-1}. Each bar represents mean ± S.E.M. ($n = 5$). One-way ANOVA statistical test was conducted to analyze significant difference among tested groups followed by Tukey–Kramer multiple comparisons test. *$P < 0.05$ *versus* normal control group. #$P < 0.05$ *versus* diabetic control group.

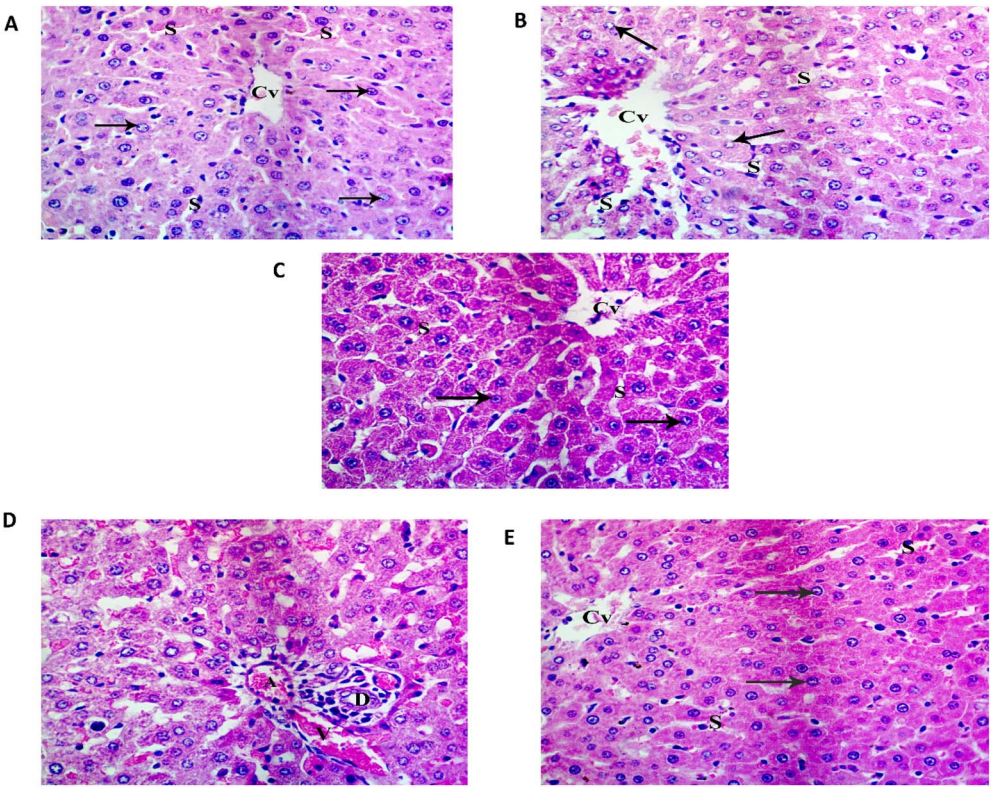

Fig. 4 Histopathological examination of liver sections (H&E staining, 400×). (A) Normal control group showing preserved hepatic architecture with radiating cords of hepatocytes (arrows), central vein (CV), and normal hepatic sinusoids (S). (B) Diabetic control group exhibiting disrupted hepatic cords, dilated sinusoids (S), and cytoplasmic vacuolations (arrows). (C) Glimepiride group showing cords of normal hepatocytes radiating from the central vein (CV) and separated by blood sinusoids (S) the hepatocytes contain eosinophilic cytoplasm and vesicular nuclei (arrows). (D) *B. daphnoides* in low dose (200 mg kg^{-1}) demonstrate mild congested hepatic artery (A), mild congested portal vein (V) and bile duct (D) lined with simple cubical epithelial cells. (E) *B. daphnoides* in high dose (400 mg kg^{-1}) showing preserved hepatic structure with normal hepatocyte arrangement, central vein (CV), and sinusoids (S), comparable to the normal control.

Bontia daphnoides may be optimal within a specific dose range.[60,61] Previous research has shown that a verbascoside-enriched extract from the leaves of *Jacaranda mimosifolia* D. Don exerted hepatoprotective effects in diabetic rats by mitigating oxidative stress and improving liver function. Treatment with verbascoside significantly reduced hepatic malondialdehyde (MDA) levels while restoring reduced glutathione (GSH) content, thereby alleviating pathological alterations in the liver. These effects were dose-dependent (10–40 mg kg^{-1}) and comparable to those of the standard antidiabetic drug pioglitazone (30 mg kg^{-1}).[62] Likewise, verbascoside isolated from *Incarvillea compacta* was reported to attenuate CCl_4-induced hepatotoxicity by enhancing superoxide dismutase activity, lowering intracellular ROS and MDA levels, and activating the nuclear factor κB (NF-κB) pathway.[38]

3.3.4.3. Histological examination of liver. Histopathological examination of liver tissues confirmed the antioxidant effect of *B. daphnoides* extract. The photomicrograph of a liver section from the normal control group (Fig. 4A) showed cords of normal hepatocytes radiating from the central vein (CV) and separated by blood sinusoids (S) the hepatocytes exhibited eosinophilic cytoplasm and vesicular nuclei (arrows). On the other hand, the photomicrograph of a liver section from diabetic rats (Fig. 4B) demonstrated marked dilatation and congestion of the central vein (CV), along with dilated and congested blood sinusoids (S). Numerous cells appeared with karyolitic nuclei (arrows). In Fig. 4C, the photomicrograph of a liver section from glimepiride-treated group showed cords of normal hepatocytes radiating from the central vein (CV) and separated by blood sinusoids (S) the hepatocytes displayed eosinophilic cytoplasm and vesicular nuclei (arrows). While that from diabetic rats treated with lower dose of *B. daphnoides* extract (200 mg kg^{-1}, Fig. 4D) showed a congested hepatic artery (A), a congested portal vein (V) and the bile duct (D) lined with simple cubical epithelial cells. Similarly, the photomicrograph of a liver section from diabetic rats treated with the plant extract in a higher dose (400 mg kg^{-1}, Fig. 4E) showed cords of normal hepatocytes radiating from the central vein (CV) and separated by blood sinusoids (S). The hepatocytes exhibited eosinophilic cytoplasm and vesicular nuclei (arrows).

4. Conclusion

Comprehensive phytochemical and biological investigations revealed *B. daphnoides* aerial parts to be rich in phenolics and flavonoids. Subsequently, ten compounds (dehydromyoporone, β-sitosterol, α-amyrin, β-sitosterol glucoside, two new γ-lactone-containing sesquiterpene, 8-acetylharpagide, verbascoside,

crenatoside, apigenin-7-*O*-glucuronide) have been isolated and identified from its hydroethanolic extract. The extract demonstrated robust antioxidant and antidiabetic activities with α-glucosidase and α-amylase inhibition surpassing or comparable to that of acarbose. Importantly, *in vivo* experiments on alloxan-induced diabetic rats clearly demonstrated the therapeutic efficacy of the extract, as it not only alleviated hyperglycemia but also attenuated oxidative stress by elevating GSH levels and reducing MDA levels, while concurrently improving the hepatic histopathology. Collectively these findings highlight *B. daphnoides* as a novel and promising source of natural compounds with dual antioxidant and antidiabetic properties, offering potential for the development of safe, plant-based therapeutic agents for management of diabetes and its associated complications.

Ethics approval and consent to participate

The study was carried out in compliance with the approved Ethical Guidelines for the Care and Use of Experimental Animals by Beni-Suef University Ethical Committee (approval no.: FPHBSU IACUC-025-006).

Author contributions

Concept and design, data acquisition, data analysis, interpretation, and final approval were created by all of the authors. The original article draft was cowritten by A. M., D. E. A., M. M. A., M. H. A. H. and M. A. Z. Isolation and structure elucidation were done by A. M., D. E. A., M. M. A., M. H. A. H. and M. A. Z. *In vivo* antidiabetic studies were carried out by M. M. A. Finally, R. M., M. A. Z., D. E. A. and M. H. A. H. contributed to supervision, technical material support, and critical revision of the manuscript.

Conflicts of interest

The authors declare that they have no competing interests.

Abbreviations

AAE	Ascorbic acid equivalent
DPPH	2,2-Diphenyl-1-picrylhydrazyl
GAE	Gallic acid equivalent
QE	Quercetin equivalent
TAC	Total antioxidant capacity
TFC	Total flavonoid content
TPC	Total phenolic content

Data availability

All data generated or analyzed during this study are included in this published article and supplementary information (SI). Supplementary information: spectral data of the isolated compounds. See DOI: https://doi.org/10.1039/d6ra00038j.

Acknowledgements

The authors would like to thank Dr Esam Rashwan, Head of the confirmatory diagnostic unit VACSERA-EGYPT, for carrying out the *in vitro* α-glucosidase and α-amylase inhibitory assays.

References

1 R. El Adaouia Taleb, N. Djebli, H. Chenini, H. Sahin and S. Kolayli, *J. Food Biochem.*, 2020, **44**, e13267.
2 D. Kalita, D. G. Holm, D. V. LaBarbera, J. M. Petrash and S. S. Jayanty, *PLoS One*, 2018, **13**, e0191025.
3 R. P. Dash, R. J. Babu and N. R. Srinivas, *Xenobiotica*, 2018, **48**, 89–108.
4 N. Kerru, A. Singh-Pillay, P. Awolade and P. Singh, *Eur. J. Med. Chem.*, 2018, **152**, 436–488.
5 B. S. Nayak, J. R. Marshall, G. Isitor and A. Adogwa, *J. Evidence-Based Complementary Altern. Med.*, 2011, **2011**, 875293.
6 L. Williams, J. Conrad, B. Vogler, H. Rosner, R. Porter, W. Setzer, E. Barton, H. Levy, S. Mika and I. Klaiber, *West Indian Med. J.*, 2007, **56**, 5.
7 C. A. Lans, *J. Ethnobiol. Ethnomed.*, 2006, **2**, 1–11.
8 U. Quattrocchi, *CRC World Dictionary of Medicinal and Poisonous Plants: Common Names, Scientific Names, Eponyms, Synonyms, and Etymology (5 Volume Set)*, CRC Press, 2012.
9 K. Lokesh, S. Kanmani, J. Adline, R. Raveen, T. Samuel, S. Arivoli and M. Jayakumar, *J. Entomol. Zool. Stud.*, 2017, **5**, 518–524.
10 A. A. Thabet, S. Moghannem, I. M. Ayoub, F. S. Youssef, E. Al Sayed and A. N. B. Singab, *Sci. Rep.*, 2022, **12**, 17707.
11 A. A. Thabet, I. M. Ayoub, F. S. Youssef, E. Al Sayed, M. S. Elnaggar, S. Moghannem, M. Korinek, R. Kalscheuer and A. N. B. Singab, *Fitoterapia*, 2025, 106743.
12 L. Hammerschmidt, V. Wray, W. Lin, E. Kamilova, P. Proksch and A. H. Aly, *Phytochem. Lett.*, 2012, **5**, 600–603.
13 N. Senthilkumar, S. Murugesan, D. S. Babu and C. Rajeshkannan, *Int. J. Innov. Res. Sci. Eng. Tech.*, 2014, **3**, 10176–10179.
14 C.-C. Chang, M.-H. Yang, H.-M. Wen and J.-C. Chern, *J. Food Drug Anal.*, 2002, **10**(3), 178–182.
15 Y. Velioglu, G. Mazza, L. Gao and B. Oomah, *J. Agric. Food Chem.*, 1998, **46**, 4113–4117.
16 T. Kulisic, A. Radonic, V. Katalinic and M. Milos, *Food Chem.*, 2004, **85**, 633–640.
17 P. Prieto, M. Pineda and M. Aguilar, *Anal. Biochem.*, 1999, **269**(2), 337–341.
18 D. Pant, B. Aryal, D. Pun, S. Sharma and G. P. Joshi, *Biodiversitas*, 2021, **22**(3), 1187.
19 H. E. Lebovitz, *Endocrinol. Metab. Clin. North Am.*, 1997, **26**, 539–551.
20 M. F. A. Bakar, M. Mohamed, A. Rahmat and J. Fry, *Food Chem.*, 2009, **113**, 479–483.
21 A. Bhatia, B. Singh, R. Arora and S. Arora, *BMC Complementary Altern. Med.*, 2019, **19**, 74.

22 M. N. Wickramaratne, J. Punchihewa and D. Wickramaratne, *BMC Complementary Altern. Med.*, 2016, **16**, 466.
23 P. Ridgway, *Rapp. ISTISAN*, 2002, **41**, 27–31.
24 O. L. Sheriff, O. Olayemi, A. O. Taofeeq, K. E. Riskat, D. E. Ojochebo and A. O. Ibukunoluwa, *J. Bangladesh Soc. Physiol.*, 2019, **14**, 56–62.
25 Y. Togashi, J. Shirakawa, T. Okuyama, S. Yamazaki, M. Kyohara, A. Miyazawa, T. Suzuki, M. Hamada and Y. Terauchi, *Sci. Rep.*, 2016, **6**, 25465.
26 A. Mishra, *Int. J. Basic Clin. Pharmacol.*, 2019, **8**(3), 589–594.
27 J. D. Bancroft and M. Gamble, *Theory and Practice of Histological Techniques*, Elsevier Health Sciences, 2008.
28 J. Li, X. Huang, X. Du, W. Sun and Y. Zhang, *Nat. Prod. Res.*, 2009, **23**, 775–780.
29 S. Elhawary, M. H. Hassan, S. I. El-Desoucky, A. Elwekeel, E. I. Mohamed, U. R. Abdelmohsen, H. M. Hassan and R. Mohammed, *Rev. Bras. Farmacogn.*, 2023, **33**, 432–437.
30 T. Peshin and H. Kar, *Br. J. Pharm. Res.*, 2017, **16**(4), 1–8.
31 G. Renda, M. Kadıoğlu, M. Kılıç, B. Korkmaz and H. Kırmızıbekmez, *Hum. Exp. Toxicol.*, 2021, **40**(12), S676–S683.
32 R. Miranda, G. Silva, L. Duarte, I. Fortes and S. V. Filho, *Magn. Reson. Chem.*, 2006, **44**, 127–131.
33 P. Naidu, K. Kumar, S. Sujatha and M. Rao, *J. Pharm. Res.*, 2012, **5**(4), 1970–1973.
34 N.-R. Shin, A. Y. Lee, J.-H. Song, S. Yang, I. Park, J.-O. Lim, T.-Y. Jung, J.-W. Ko, J.-C. Kim and K. S. Lim, *Phytomedicine*, 2020, **67**, 153159.
35 D. Gao, V. Le Ba, R. Rustam, C. W. Cho, S. Y. Yang, X. D. Su, Y. H. Kim and J. S. Kang, *Prep. Biochem. Biotechnol.*, 2021, **51**(4), 395–404.
36 A. Delazar, S. Asnaashari, E. Nikkhah and P. Asgharian, *Res. Pharm. Sci.*, 2019, **14**(3), 263–272.
37 F. R. da Silva, F. E. Rodrigues, A. R. Gomes, A. Arriaga, J. Mafezoli, T. L. Lemos, M. Almeida, G. M. Santiago, R. Braz-Filho and J. G. da Costa, *Quim. Nova*, 2014, **37**, 1474–1478.
38 T. Shen, X. Li, W. Hu, L. Zhang, X. Xu, H. Wu and L. Ji, *J. Korean Soc. Appl. Biol. Chem.*, 2015, **58**, 617–625.
39 S.-V. Luca, M. E. Czerwińska, L. Marcourt, A. Miron, A. C. Aprotosoaie, N. Ciocarlan, J.-L. Wolfender, S. Granica and K. Skalicka-Woźniak, *Phytochem. Lett.*, 2019, **31**, 249–255.
40 N.-H. Du, R.-L. Xiong, T.-T. Zhu, X.-Y. Liu, J.-Z. Zhang, J. Fu, H.-L. Wang, H.-X. Lou and A.-X. Cheng, *J. Nat. Prod.*, 2024, **87**, 228–237.
41 T. Gyeltshen, B. J. Deans, C. C. Ho, N. L. Kilah, J. A. Smith and A. C. Bissember, *J. Nat. Prod.*, 2023, **86**, 1584–1595.
42 R. J. Chinnock, E. L. Ghisalberti and P. R. Jefferies, *Phytochemistry*, 1987, **26**, 1202–1203.
43 P. Khound, H. Sarma, P. P. Sarma, U. K. Jana and R. Devi, *ACS Omega*, 2023, **8**, 20360–20369.
44 L. Wu, M. I. Georgiev, H. Cao, L. Nahar, H. R. El-Seedi, S. D. Sarker, J. Xiao and B. Lu, *Med. Res. Rev.*, 2020, **40**, 2605–2649.
45 K. Kamalakararao, V. Gopalakrishnan, Z. Hagos, Y. Satyaprasad and K. C. Karri, *Drug Intervention Today*, 2018, **10**, 1142–1146.
46 M. Akmal, P. Patel and R. Wadhwa, in *StatPearls [Internet]*, StatPearls Publishing, 2024.
47 Q. Liu, H.-J. Hu, P.-F. Li, Y.-B. Yang, L.-H. Wu, G.-X. Chou and Z.-T. Wang, *Phytochemistry*, 2014, **103**, 196–202.
48 L. N. Tuong Vi, N. N. Tuan, Q. T. Hung, P. T. N. Trinh, T. T. Danh, N. Thao Ly, V. N. Thao and L. T. Dung, *Nat. Prod. J.*, 2022, **12**, 63–68.
49 Y.-l. Liu, W.-j. He, L. Mo, M.-f. Shi, Y.-y. Zhu, S. Pan, X.-r. Li, Q.-m. Xu and S.-l. Yang, *J. Ethnopharmacol.*, 2013, **149**, 431–437.
50 X.-D. Mao, G.-X. Chou, S.-M. Zhao and C.-G. Zhang, *Molecules*, 2016, **21**, 1749.
51 A. Rohilla and S. Ali, *Int. J. Res. Pharm. Biomed. Sci.*, 2012, **3**, 819–823.
52 S. Lenzen, *Diabetologia*, 2008, **51**, 216–226.
53 G. Muller, *Curr. Med. Chem.: Immunol., Endocr. Metab. Agents*, 2005, **5**, 499–518.
54 A. Boudjelal, C. Henchiri, L. Siracusa, M. Sari and G. Ruberto, *Fitoterapia*, 2012, **83**, 286–292.
55 T. Morikawa, K. Ninomiya, M. Imamura, J. Akaki, S. Fujikura, Y. Pan, D. Yuan, M. Yoshikawa, X. Jia and Z. Li, *J. Nat. Med.*, 2014, **68**, 561–566.
56 B. Ahmed, A. J. Al-Rehaily, T. A. Al-Howiriny, K. A. El-Sayed and M. S. Ahmad, *Biol. Pharm. Bull.*, 2003, **26**, 462–467.
57 A. Yesupatham and R. Saraswathy, *Biochem. Biophys. Rep.*, 2025, **43**, 102069.
58 P. Newsholme, K. N. Keane, R. Carlessi and V. Cruzat, *Am. J. Physiol.: Cell Physiol.*, 2019, **317**, C420–C433.
59 A. Avignon, M. Hokayem, C. Bisbal and K. Lambert, *Nutrition*, 2012, **28**, 715–721.
60 J. Bouayed and T. Bohn, *Oxid. Med. Cell. Longevity*, 2010, **3**, 228–237.
61 R. A. Guneidy, E. R. Zaki, A. A. M. Gad, N. S. E.-D. Saleh and A. Shokeer, *Prev. Nutr. Food Sci.*, 2022, **27**, 282.
62 S. A. El-Marasy, S. M. El-Shenawy, F. A. Moharram and N. A. El-Sherbeeny, *Open Access Maced. J. Med. Sci.*, 2020, **8**, 125–133.